Journal of Alloys and Compounds 488 (2009) 437–441

Contents lists available at ScienceDirect

Journal of Alloys and Compounds

journal homepage: www.elsevier.com/locate/jallcom

Structural and magnetotransport properties of $La_{0.67}Sr_{0.33}MnO_z$ thin films prepared by metal–organic decomposition under different annealing process

Xiangrong Zhu[a,b,*], Honglie Shen[c], Zhengxia Tang[c], Koichi Tsukamoto[d], Takeshi Yanagisawa[d], Mamoru Okutomi[d], Noboru Higuchi[d]

[a] School of Urban Development and Environmental Engineering, Shanghai Second Polytechnic University, 2360 Jinhai Road, Shanghai 201209, PR China
[b] State Key Laboratory of Functional Materials for Informatics, Shanghai Institute of Microsystem and Information Technology, Chinese Academy of Sciences, 865 Changning Road, Shanghai 200050, PR China
[c] College of Materials Science & Technology, Nanjing University of Aeronautics & Astronautics, Nanjing 211100, PR China
[d] National Institute of Advanced Industrial Science and Technology, 1-1-4 Umezono, Tsukuba, Ibaraki 305-8568, Japan

ARTICLE INFO

Article history:
Received 27 June 2009
Received in revised form 23 August 2009
Accepted 25 August 2009
Available online 8 September 2009

PACS:
75.47.−m
75.47.GK
81.15.−z
68.55.−a

Keywords:
LSMO film
Metal–organic decomposition
Structure
Magnetotransport

ABSTRACT

$La_{0.67}Sr_{0.33}MnO_z$ (LSMO) thin films were prepared by means of metal–organic decomposition on amorphous quartz substrates under different annealing process. X-ray diffraction spectra show that proper crystallization temperature of the films is beyond 873 K and all samples annealed at 953 K or above present polycrystalline structure with [2 0 2] preferred orientation. Higher annealing temperature or longer annealing time lead to growth of larger grain. Regardless of the difference of grain size, all polycrystalline films present similar and steady magnetotransport properties, such as enhanced magnetoresistance (MR) effect below metal–insulator transition temperature and approximate MR ratio under same applied field, which were ascribed to the porous structural characteristics in the films observed by an atomic force microscope. Additionally, at room temperature the resistivity of each polycrystalline film presents linear change over wide range of applied field and get MR ratio near 5% under 10 kOe field.

1. Introduction

As one kind of colossal magnetoresistance (CMR) manganites, for almost two decades $La_{0.67}Sr_{0.33}MnO_3$ (LSMO) has been drawing intensive interest on account of its high spin polarization and excellent magnetotransport properties such as high MR ratio near room temperature (RT) which is critical to its applications on highly sensitive magnetic sensors, magnetic random access memory, etc [1–4]. Structural characteristics of the CMR materials play very important roles in the magnetotransport properties. Unlike single crystal materials, polycrystalline materials would present the so-called large low-field MR effect. Namely, CMR ratio would change steeply over low-field range below Curie temperature, which is correlated with the spin-polarized intergrain tunneling and the spin-dependent scattering at interfaces or grain boundaries [1–3,5]. In addition, for polycrystalline CMR materials with porous structural characteristics, the porosity would weaken the link between grains and then result in an enhanced MR behavior [6]. Namely, over the temperature range below metal–insulator transition, the CMR ratio would still increase with decreasing temperature when a magnetic field is applied.

Hitherto $La_xSr_{1-x}MnO_3$ thin films have been mainly prepared by pulsed laser deposition (PLD) [7,8], rf or dc sputtering [9,10], metal–organic chemical vapor deposition (MOCVD) [11] and molecular beam epitaxy [12]. All these methods require large, complex and expensive equipment. In contrast, solution deposition methods for oxide films such as sol–gel and metal–organic decomposition (MOD) do not need large equipment, and the routine of preparing films by these methods is relatively simple. Once we have reported the successful MOD growth of $La_{0.67}Ca_{0.33}MnO_z$ and $La_{0.67}Ba_{0.33}MnO_z$ films and discussed their structural characteristics and CMR properties in detail [13,14].

* Corresponding author at: School of Urban Development and Environmental Engineering, Shanghai Second Polytechnic University, 2360 Jinhai Road, Shanghai 201209, PR China. Tel.: +86 21 50215021x8536; fax: +86 21 50217725.
E-mail address: zhuxiangrong71@126.com (X. Zhu).

0925-8388/$ – see front matter © 2009 Elsevier B.V. All rights reserved.
doi:10.1016/j.jallcom.2009.08.151

Table 1
The MOD annealing process corresponding to coded sample.

Sample code	LSM0	LSM1	LSM2	LSM3	LSM4	LSM5	LSM6
Annealing process	873 K, 50 min	953 K, 50 min	993 K, 50 min	1033 K, 50 min	1073 K, 50 min	993 K, 80 min	993 K, 100 min

Usually the structural characteristics of CMR films are determined by the preparation technique such as the deposition methods, working pressure, substrate temperature and the type of substrates. Recently Sahu [10] has studied the effect of substrate temperature ranging from 600 °C (873 K) to 750 °C (1023 K) on the structural, magnetic and transporting properties of $La_{0.7}Sr_{0.3}MnO_3$ films on Si (1 0 0) prepared by dc magnetron sputtering. The results revealed that all films presented metal–insulator transition near 250 K and the films deposited at 650 °C (923 K) have the best crystalline quality and the highest Curie temperature (T_C) of 300 K.

In this article, we reported the MOD growth of $La_{0.67}Sr_{0.33}MnO_z$ films on amorphous quartz under different annealing process and investigated their structural characteristics and magnetotransport properties. Here, the oxygen composition is marked as z because the MOD annealing technique was conducted in air, which would result in the minor deviation of oxygen.

2. Experimental

In our MOD experiment, the starting solutions, $LaO_{1.5}$, $MnO_{1.5}$ and SrO, were purchased from an agency of Symetrix Corporation in Japan. Their molar concentrations were 0.1–0.5 mol/l. According to the nominal composition of $La_{0.67}Sr_{0.33}MnO_z$, the above solutions were mixed in such a way that the molar ratio of La:Sr:Mn was consistent with 2:1:3. The mixed solutions were used as precursor solutions, which were spin-coated on clean amorphous quartz substrates to form wet films. Then the wet films were baked in air at 473 K for 10 min. In order to increase the film thickness, the above process of preparing and baking gel films was repeated twice. After the baking, the gel films were annealed in air under different conditions.

For the sake of studying the effects of annealing process, two groups of samples were prepared. As listed in Table 1, for samples LSM0, LSM1, LSM2, LSM3 and LSM4, which constituted Group 1, the annealing temperature was raised from 873 K to 1073 K with the same 50 min annealing time. For samples LSM5 and LSM6, their annealing temperature was 993 K, same as LSM2, and the annealing time was prolonged to 80 min and 100 min separately. LSM2, LSM5 and LSM6 constituted Group 2. It should be noticed that LSM2 belonged to either Group 1 or Group 2. After annealing all the samples were slowly cooled down to room temperature (RT) by shutting off the heat treatment system.

LSM2 was chosen as one typical sample for conducting measurement of Rutherford backscattering spectra, which showed that the composition of the metallic elements in the film varied from that of the corresponding concocted solutions by about 5% and the thickness of the films was about 1200 Å. For all samples, the crystalline structure was determined by an X-ray diffractometer (XRD). The surface morphologies were observed by an atomic force microscope (AFM). The magnetotransport properties were measured by means of standard four-probe technique over a temperature range from 77 K to RT while the probe current was parallel to the longitudinal direction of the films and the magnetic field was applied along the current direction.

3. Results and discussion

Fig. 1 shows the XRD spectra of all LSMO samples. First, compared to those of other samples, the XRD spectrum of LSM0 displays only one very weak [2 0 2] peak, implying that the crystallization of the film would become difficult below 873 K annealing temperature. The several indexed peaks in the XRD spectra from LSM1 to LSM6 reveal the typical polycrystalline perovskite structural characteristics. Secondly, the [2 0 2] peaks are much higher than the other indexed peaks, indicating the [2 0 2] preferred orientation of the films, which is similar to the $La_{0.67}Ba_{0.3}MnO_z$ films on amorphous quartz grown by MOD [13]. Thirdly, for Group 1 samples, the strength of [2 0 2] peaks from LSM1 to LSM4 presents an increasing tendency. For Group 2 samples, the strength of [2 0 2] peaks successively increases from LSM2, LSM5 to LSM6. These results imply the grain size of the films would become larger when the annealing temperature is raised or the annealing time is prolonged. Finally, for all samples except LSM0, the positions of main peaks [2 0 2] are very close, located near 32.85° (2θ), indicating that the samples have very similar lattice constants. In fact, for $La_{1-x}Sr_xMnO_z$, the lattice structure is determined by x, the content of Sr [15]. Thus for the polycrystalline samples from LSM1 to LSM6, different annealing process would not change the lattice constants.

The 5 μm × 5 μm AFM images of the surface morphology of all polycrystalline LSMO films are displayed in Fig. 2. It can be observed that, for each sample, near round particles were grown smoothly and uniformly on the substrate. The size of the particles ranges from 200 nm to 300 nm. At the same time, the structure of each film seems a bit porous, meaning the films are not dense and the grain boundaries are weakly linked. Furthermore, the surface root mean square (RMS) roughness of each sample presents regular change. On the one hand, for Group 1 samples, the size of surface RMS roughness increases with annealing temperature, from 6.8 nm for LSM1 to 9.3 nm for LSM4. On the other hand, for Group 2 samples, under the same 993 K annealing temperature the size of surface RMS roughness becomes larger with longer annealing time, from 8.2 nm for LSM2 to 9.3 nm for LSM6. The surface roughness of the film reflects the grain size. Thus the above results further indicate that, the grain size of the films would increase with annealing temperature or annealing time, as discussed in XRD results, which is consistent with the classical principles of crystallization kinetics.

The measurement of magnetotransport properties was conducted for all samples except LSM0 because LSM0 hardly presents polycrystalline structure and exhibits almost entirely insulator property. For samples LSM1 to LSM6, the temperature dependences of resistivity under zero field, 8 kOe field and corresponding MR from 77 K to RT are plotted in Fig. 3. MR ratio is defined as $[\rho_0 - \rho_H]/\rho_0 \times 100\%$, where ρ_0 is the resistivity under zero field and ρ_H the resistivity under applied field. Here, H is 8 kOe. Fig. 3 shows that all samples present similar magnetotransport properties. First, the resistivity–temperature dependence of each sample under zero

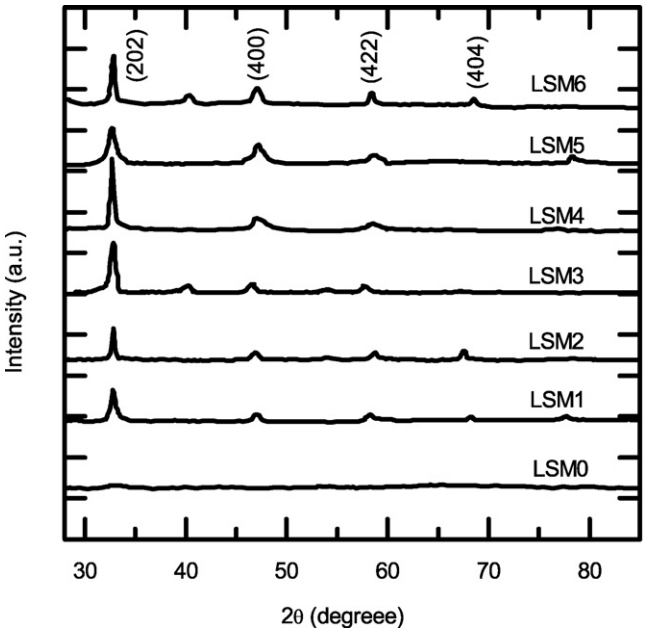

Fig. 1. The XRD spectra of all LSMO films under different annealing process.

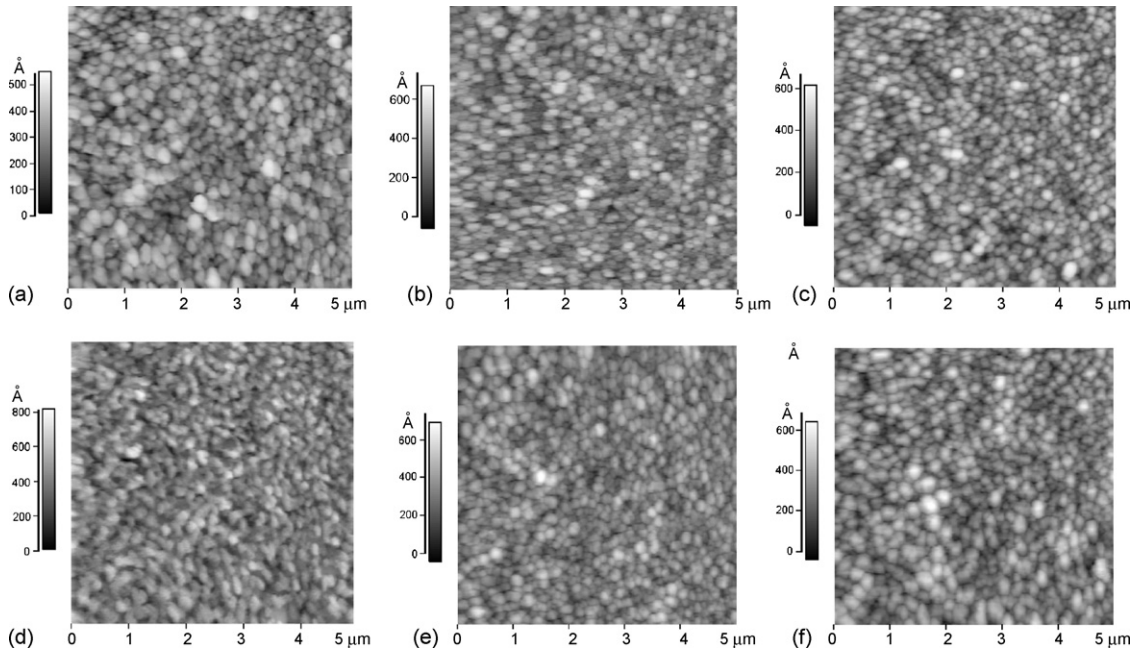

Fig. 2. The 5 μm × 5 μm AFM images of surface morphology of all polycrystalline LSMO films. (a) LSM1, (b) LSM2, (c) LSM3, (d) LSM4, (e) LSM5 and (f) LSM6.

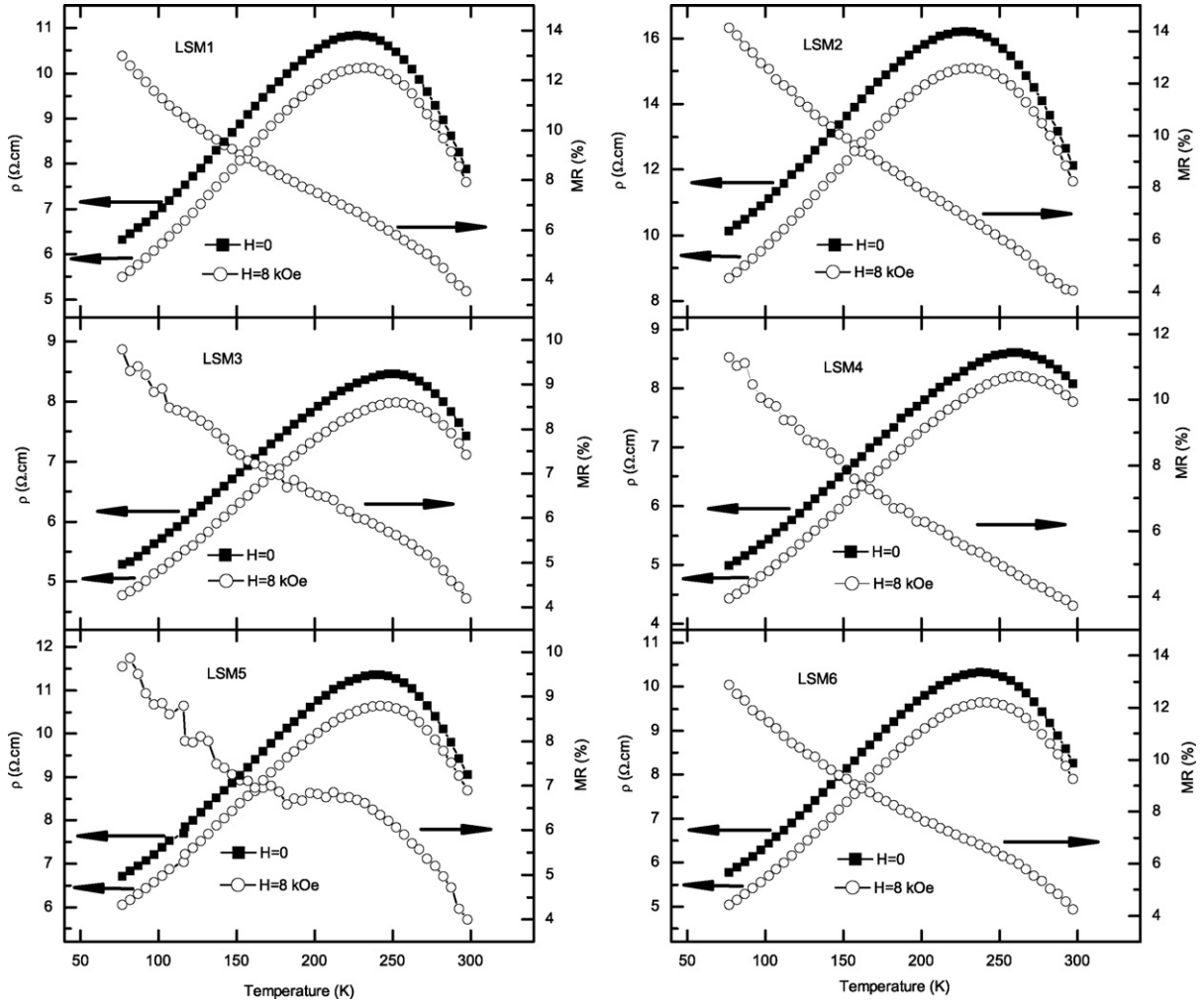

Fig. 3. Temperature dependences of resistivity under zero field, 8 kOe field and corresponding MR for the polycrystalline LSMO films under different annealing process.

Table 2
The data of metal–insulator transition temperature T_p of each $La_{0.67}Sr_{0.33}MnO_z$ film.

Sample code	LSM1	LSM2	LSM3	LSM4	LSM5	LSM6
T_p	227 K	227 K	252 K	257 K	242 K	237 K

field shows only one peak, namely the typical metal–insulator transition peak. The data of transition peak temperature T_p are listed in Table 2. For Group 1 samples, the T_p of LSM4 is highest, 257 K and of LSM1 is lowest, 227 K. For Group 2 samples, the T_p of LSM5 and LSM6 is just 10–15 K higher than that of LSM2, which means higher annealing temperature or longer annealing time lead to higher T_p. The difference of T_p might result from the grain size effect [10]. It should be pointed that, for LSMO, its Curie temperature T_C is always dozens of Kelvin higher than room temperature [1]. So the T_p of each sample is far lower than T_C by 100 K more or less. Under applied 8 kOe field, the resistivity is decreased and the temperature of resistivity peak becomes a bit higher than corresponding T_p. Secondly, the MR ratio of each sample under 8 kOe filed monotonously increases with the temperature decreasing from RT to 77 K, and no MR peak appears near T_p, exhibiting a strong enhanced MR effect over the temperature range below T_p. Thirdly, the difference of MR ratio of the samples is not significant. At 77 K, the MR ratio of the samples varies from 10% to 14%, and at 297 K (RT) MR ratio is close to 4%. Except the differences of the T_p, the above results reveal steady magnetotransport properties of the samples despite their grain size caused by different annealing process.

The magnetotransport properties of our samples are quite different from those of $La_{0.7}Sr_{0.3}MnO_3$ films reported by Sahu [10]. First, the $La_{0.7}Sr_{0.3}MnO_3$ films present approximate T_p range to our samples. However, for these samples, besides the metal–insulator transition peak, another resistance peak appears over the temperature range from 200 K to T_p. Secondly, the MR-temperature dependence of each $La_{0.7}Sr_{0.3}MnO_3$ film displays a MR peak near T_p. Enhanced MR behavior just occurs over lower temperature range from about 170 K to 100 K. Thirdly, for the $La_{0.7}Sr_{0.3}MnO_3$ films, the MR ratio is quite different from each other under same applied field. In general, there exist obvious differences of magnetotransport properties among the above $La_{0.7}Sr_{0.3}MnO_3$ films.

The great difference of magnetotransport properties between our samples and above $La_{0.7}Sr_{0.3}MnO_3$ films might originate from the different structural characteristics between the two kinds of samples. As reported by Sahu [10], interfacial layers in the grain boundaries are observed by scanning electronic microscope (SEM) in the $La_{0.7}Sr_{0.3}MnO_3$ films, which play key roles in spin-dependent tunneling or scattering [16,17]. The contribution of interfacial layers to spin-dependent tunneling or scattering are sensitive to grain size, which would lead to sensitive magnetotransport properties to grain size controlled by substrate temperature during the dc magnetron sputtering. Similar strong effects of grain size on mangetotransport properties were also observed in polycrystalline $La_{0.8}Sr_{0.2}MnO_3$ [18]. For our samples, the AFM images show their structure is a bit porous. These structural defects of porosity could cause weak-linked grain boundaries, where the alignment of spins becomes easy and thus strong enhanced MR behavior occurs below metal–insulator transition temperature [6]. It can be deduced that, defects of porosity are intrinsic structural characteristics of our samples and are not sensitive to the grain size. The magnetotransport behaviors would be dominated by structural defects of porosity. Thus for our samples, the magnetotransport properties become similar and steady regardless of the differences of grain sizes.

The field dependences of resistivity of the polycrystalline $La_{0.67}Sr_{0.33}MnO_z$ films were also investigated at RT (297 K). As shown in Fig. 4, for each sample, when the applied filed H is scanned from +10 kOe to −10 kOe and back, the normalized resistivity ρ_H/ρ_{max} changes linearly over wide field range. Here, ρ_{max} is the maximum resistivity that would not appear at zero field but near the coercive field of the corresponding film due to the hysteresis effect of resistivity as mentioned below. It could be calculated that under 10 kOe field, the MR ratio of each sample is near 5%. For LSM2, the enlarged normalized resistivity-field dependence curve

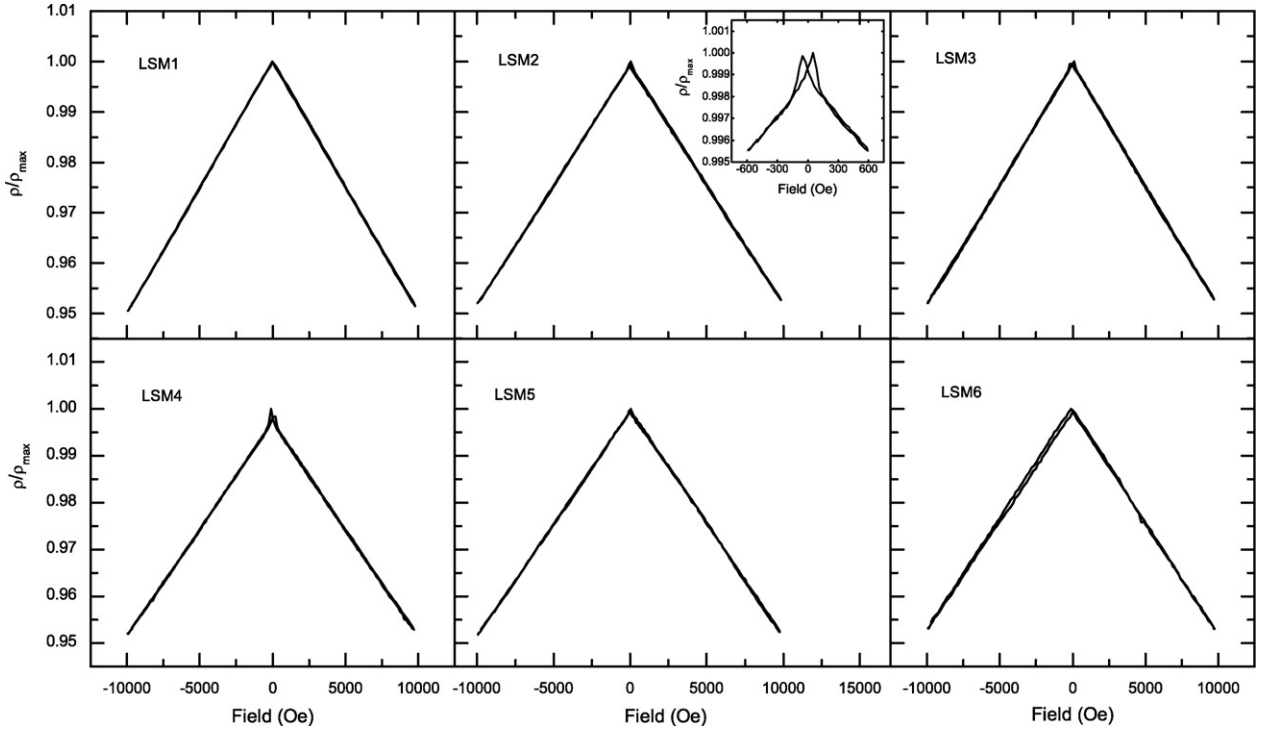

Fig. 4. Resistivity normalized to its maximum for the polycrystalline LSMO films at 297 K (RT) as a function of applied filed which is changed from +10 KOe to −10 kOe and back.

below 600 Oe is simultaneously embedded in Fig. 4. Considerable low-field MR behavior and hysteresis of resistivity is observed in this embedded curve. According to the study by Hwang et al. [1], the low-field MR effect occurs when the polycrystalline CMR materials keep ferromagnetism and would decline from low temperature to high temperature. Since the T_C of LSMO is dozens of Kelvin higher than RT, the appearance of low-filed MR effect at RT could be understood. The hysteresis of resistivity reflects the close correlation between magnetotransport and magnetization. Near the coercive field the maximum resistivity would appear [19]. Additionally, it is worth pointing out that, the similar MR-field dependences of all the samples at RT further reveal the steady magnetotransport properties resulting from the porous structural characteristics despite of the different annealing process, and the linearity of MR over wide range of magnetic filed and considerable MR ratio at RT should be significant to the application for LSMO films.

4. Conclusion

In summary, $La_{0.67}Sr_{0.33}MnO_z$ thin films were synthesized by means of MOD under different annealing conditions. The XRD spectra showed that proper crystallization temperature for the films was beyond 873 K and all the samples annealed at 953 K or above were polycrystalline with [2 0 2] preferred orientation. The porous structural characteristics in the samples are shown by AFM. Different annealing condition just mainly led to the change of grain size. The structural defects of porosity played key roles in the mechanism of magnetotransport, leading to the enhanced MR behavior below metal–insulator transition and steady magnetotransport properties, regardless of different grain size of the samples. Moreover, at RT the resistivity of all the polycrystalline samples presents linear change over wide applied field range and get MR ratio near 5% under 10 kOe field. The above steady magnetotransport properties reveal that MOD provides with a valuable method for preparing applicable $La_{0.67}Sr_{0.33}MnO_z$ films.

Acknowledgement

The authors would like to acknowledge the financial support from Shanghai Second Polytechnic University (Fund No. XQD208011) and the Open Project of State Key Laboratory of Functional Materials for Informatics, Shanghai Institute of Microsystem and Information Technology, Chinese Academy of Sciences.

References

[1] H.Y. Hwang, S.-W. Cheong, N.P. Ong, B. Batlogg, Phys. Rev. Lett. 77 (1996) 2041.
[2] J.Y. Gu, S.B. Ogale, M. Rajeswari, T. Venkatesan, R. Ramesh, V. Radmilovic, U. Dahmen, G. Thomas, T.W. Noh, Appl. Phys. Lett. 72 (1998) 1113.
[3] S.P. Isaac, N.D. Mathur, J.E. Evetts, M.G. Blamire, Appl. Phys. Lett. 72 (1998) 2038.
[4] U. Scotti di Uccio, B. Davidson, R. Di Capua, F. Miletto Granozio, G. Pepe, P. Perna, A. Ruotolo, M. Salluzzo, J. Alloys Compd. 423 (2006) 228.
[5] A. Gupta, J. Sun, J Magn. Magn. Mater. 200 (1999) 24.
[6] X.L. Wang, S.X. Dou, H.K. Liu, M. Ionescu, B. Zeimetz, Appl. Phys. Lett. 73 (1998) 396.
[7] C.J. Lu, Z.L. Wang, C. Kwon, Q.X. Jia, Appl. Phys. 88 (2000) 4032.
[8] M.C. Terzzoli, D. Rubi, S. Duhalde, M. Villafuerte, M. Sirena, L. Steren, Appl. Surf. Sci. 186 (2002) 458.
[9] M. Sirena, N. Haberkorn, M. Granada, L.B. Steren, J. Guimpel, J. Magn. Magn Mater. 272–276 (2004) 1171.
[10] D.R. Sahu, Appl. Surf. Sci. 255 (2008) 1870.
[11] S. Pignard, H. Vincent, J.P. Senateur, P.H. Giauque, Thin Solid Films 347 (1997) 161.
[12] Z. Yang, L. Sun, C. Ke, X. Chen, W. Zhu, O. Tan, J. Cryst. Growth 311 (2009) 3289.
[13] X.-R. Zhu, H.-L. Shen, S.-C. Zou, K. Tsukamoto, T. Yanagisawa, M. Okutomi, N. Higuchi, Appl. Surf. Sci. 161 (2000) 203.
[14] X.-R. Zhu, H.-L. Shen, T. Li, G.-X. Li, S.-C. Zou, K. Tsukamoto, T. Yanagisawa, M. Okutomi, A. Obara, Thin Solid Films 375 (2000) 228.
[15] A. Urushibara, Y. Moritomo, T. Arimo, A. Asamitsu, G. Kido, Y. Tokura, Phys. Rev. B 51 (1995) 14103.
[16] K. Steenbeck, T. Eick, K. Kirsch, H.G. Schmidt, E. Steinbeib, Appl. Phys. Lett. 73 (1998) 2506.
[17] E. Steinbeib, K. Steenbeck, T. Eick, K. Kirsch, Vacuum 58 (2000) 135.
[18] P. Kameli, H. Salamati, A. Aezami, J. Alloys Compd. 450 (2008) 7.
[19] K. Steenbeck, T. Eick, K. Kirsch, K. O'Donnell, E. Steinbeib, Appl. Phys. Lett. 71 (1997) 968.